

Experimental Estimate of Helical Inducer Blade Force in Cavitation Surge Condition

A. Furukawa, K. Ishizaka and S. Watanabe
Kyushu University, Fukuoka, JAPAN

Abstract

An attachment of inducer is a powerful method to improve the cavitation performance of a turbo-pump. Cavitation surge phenomena, occurring under the severe suction pressure at a partial flow rate, is focused in the present paper. Flow measurements were carried out at the inlet and outlet sections of a flat-plate helical inducer with the solidity of 2.0 and tip blade angle of 11° by using a total-head yaw-meter with a phase locked sampling method in one period of the shaft rotation or the cavitation oscillation. Time variation of the flow distributions during the oscillation is clarified with observed cavitation behaviors. After these results are compared with those in conditions just before and after the oscillations, the fluctuating blade forces are estimated from the blade to blade distributions of casing wall pressures measured in these conditions.

1. Introduction

The shaft rotational speed of turbo-pumps, used in various industrial fields, become higher and higher from restrictions in the compact structure and a narrower space of the installation. A current demand for pump designers is how to improve the suction performance of pumps. A solution to obtain higher suction performance is an attachment of inducer in front of main impellers (Takamatsu(1975)).

Various modes of cavitation induced oscillations, however, occur in the certain range of partial flow rates and low NPSH (Acosta(1958), Tsujimoto(1997)). Especially a harmful oscillation, which causes a trouble of the vibrating pipeline and equipment, is known as the cavitation surge with very low frequency. To avoid this trouble, some devices have been proposed such as a casing treatment to reduce a back flow at tip region of inducer inlet (Jacobsen(1971)) and many kinds of accumulators to damp the pressure fluctuation in suction pipe (Rubin(1970)). However it is necessary to use these devices carefully to suppress the oscillation and the response of the flow control and also the efficiency in the normal range of flow rate might be sacrificed. On the other hand, a mathematical model has been proposed to estimate its occurrence (Watanabe(1978)) and using various models these cavitation-induced oscillations become possible to be predicted quantitatively. An idea of advance detector system of cavitation surge precursor has been also proposed (Ishizaka(1998)). It is not sufficient to understand the behavior of cavitation surge oscillations.

The purpose of the present study is to clarify the behavior of the cavitation induced oscillation in a flat-plate helical inducer with the solidity of 2.0 and tip blade angle of 11° by flow measurement and cavitation visualization. Then the fluctuating blade forces are estimated from the blade to blade distributions of casing wall pressures measured in conditions before and after the oscillations.

2. Experimental Apparatus

Figures 1 and 2 show a closed water flow loop used and a cross-sectional view of test section, respectively. The suction pipe has the inner diameter of 125mm and the length of 9.5m from the tank to the upstream straight vanes and the discharge pipe has 50mm diameter and 2.9m length from the water circulation (booster) pump outlet to the tank. On the discharge piping line, a strainer, an electromagnetic

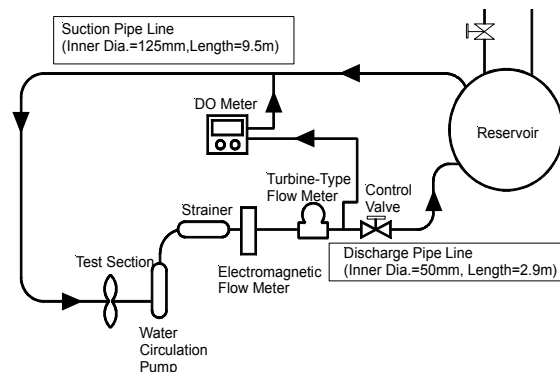


Fig.1 Test loop of water flow

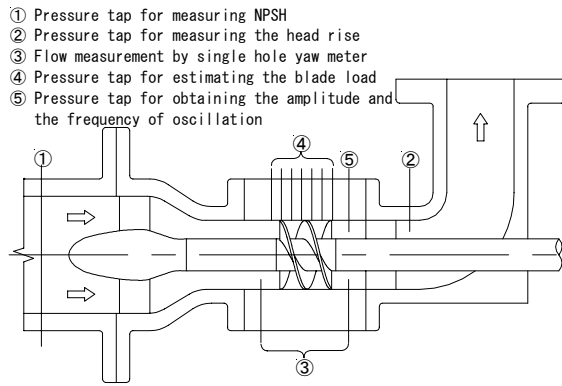


Fig.2 Test section

in Fig.2 with taking account of guide vane losses and the change of dynamic head. The NPSH was calculated from the pressure at the section ① with taking account of guide vane loss and water temperature. The casing wall pressures were measured at the inducer outlet position ⑤ and the seven axial positions of ④. The radial distributions of flow were also measured at the inducer inlet and outlet sections of ③ with a single-hole yaw-meter. These instantaneous pressure measurements were performed by using a high response sensor with a phase-locked sampling method in one period of the shaft rotation in no cavitation oscillating condition or of the cavitation oscillation with the trigger signal of measured pressure at the section ⑤ in the cavitation oscillating condition. The mean pressure at each phase position in one period of the rotation or the cavitation oscillation was obtained by averaging sampling signals of 120 shaft rotations. The silicon oil was put into the conduit pipe from the pressure hole to the sensor to avoid the destruction due to cavitation collapse impulse force. It is verified experimentally that the response frequency of the sensor has 1.2kHz for wall pressure measuring sensor and 150Hz for flow distribution measuring sensor, respectively, with no damping and no delay of signal. The scheme of flow measurement with a single-hole yaw-meter in a periodic flow is the same as the measurement with a three-holes yaw-meter by changing the pressure hole direction (Takahara, 1989). The cavitation behavior was observed by video-camera equipment of 30fps (normal) and 1000fps (high speed) with a synchronized strobo-light through the transparent casing wall.

It is known that the mode and the frequency of cavitation induced oscillations are varied with the solidity of inducers (Ishizaka, 1990). In the present paper, a two bladed flat-plate helical inducer with a hub-tip ratio of 0.469 (the tip diameter of 64mm and the tip clearance of 0.5mm), having the solidity of $\sigma_t=2.04$ and the blade angle of $\beta_t=11.25^\circ$ at the inducer tip, was tested. Test was carried out at flow coefficient of $\phi_t=0.017$ or flow rate ratio $m=\phi_t/\tan\beta_t=0.086$. This inducer

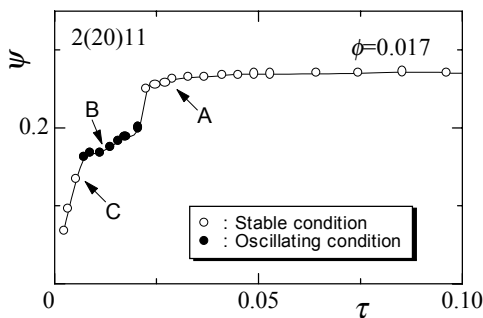


Fig.3 Head deterioration curve due to cavitation

flow meter, a turbine-type one and a control valve are installed. The booster pump was operated when the inducer head is not high enough to circulate water in the loop. It is verified experimentally that the booster pump operation has no influence on the cavitation surge phenomena of inducers. Cavitation tests were performed after pre-operation under cavitating conditions of low NPSH for a long time instead of deaeration. The rotational speed, N , was kept 5000rpm constant with the deviation of 0.2%. The mean flow rate, Q , is measured by a turbine-type flow meter and its fluctuation by an electromagnetic one with the error less than 2%. The inducer head, H_i , was evaluated from the wall pressure difference between the sections ① and ②

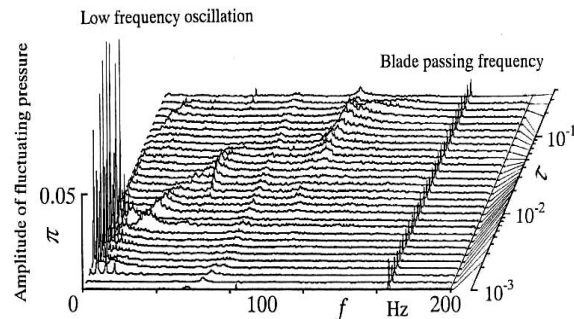


Fig.4 Spectrum analysis of casing wall pressure at inducer outlet

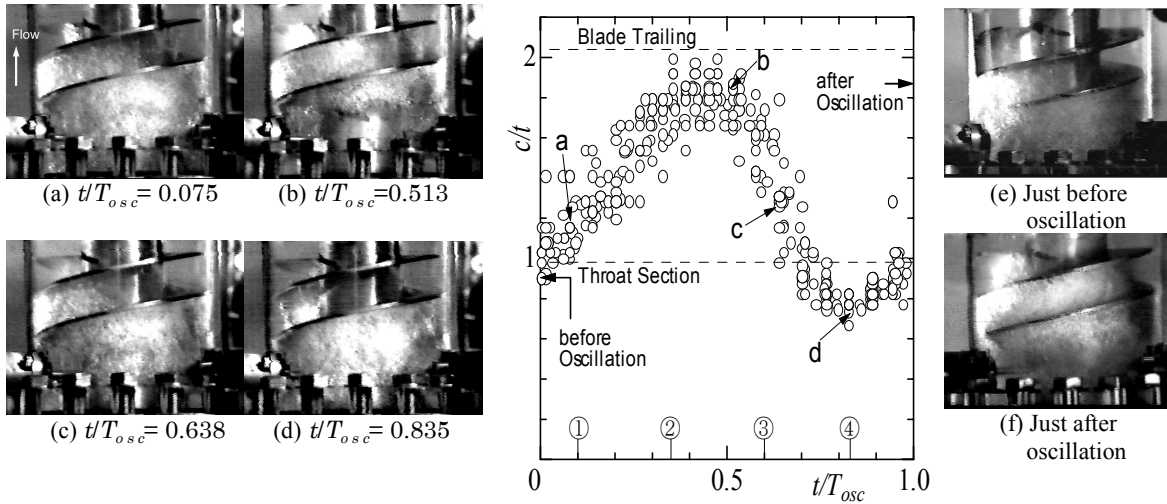


Fig.5 Time variation of cavitation behaviors during oscillation

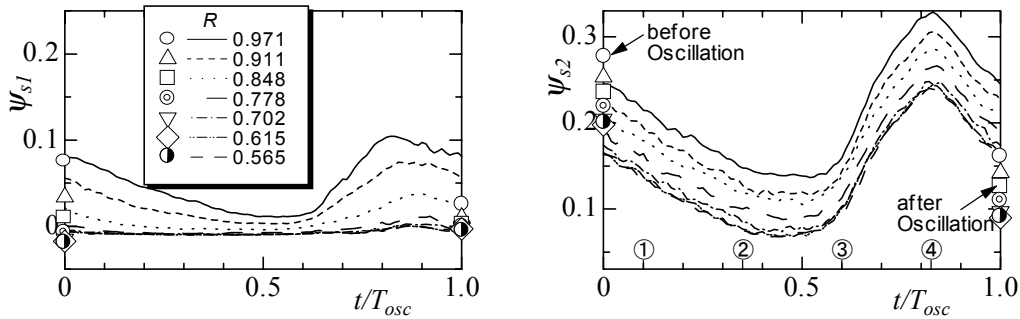


Fig.6 Time variation of static pressures during oscillation

is denoted as IND2(20)11 by standing for the blade number of 2, tip solidity of 2.0 and tip blade angle of 11° in order.

3. Test results and discussions

3.1 Cavitation characteristics

Figure 3 shows a head deterioration curve due to cavitation in various NPSH conditions at $\phi=0.017$ and Fig.4 depicts a spectrum analysis of inducer outlet pressure. Here, ψ , τ and π are head coefficient, dimensionless NPSH and amplitude of static-head fluctuation, normalized by (U_i^2/g) (U_i : the rotational speed of inducer tip, g : the acceleration of gravity), respectively and f is the frequency of head fluctuation. At high NPSH where the tip vortex and weak back flow cavitations are observed, the broad band fluctuation, might be caused by a unstable behavior of three-dimensional back flow, appears in the range of about 1.08 times the shaft rotating frequency in Fig.4. As NPSH is decreased, its fluctuation disappears. Then the fluctuation with low frequency of 2Hz (within $\pm 3.5\%$) occurs at $\tau < 0.03$ and the inducer head is gradually deteriorated. It is defined in the present paper that cavitation surge occurs when the amplitude of head fluctuation with low frequency becomes higher than that of blade passing frequency. The occurring regions of cavitation surge oscillation are illustrated as solid symbols in Fig.3. With further decreasing NPSH, the cavitation surge oscillation disappears and the inducer head goes to the breakdown.

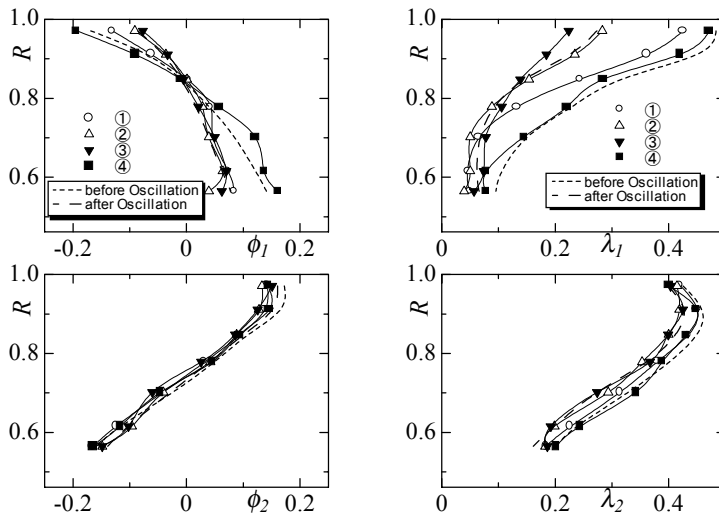


Fig.7 Time variation of radial distributions of flow velocity during oscillation

3.2 Flow and cavitation behaviors in low frequency oscillation condition

Flow measurement at the inducer inlet and outlet sections of ③ in Fig.2 were carried out at the points of **A**~**C** shown on the head deterioration curve in Fig.3. The point of **B** is in the oscillation condition with almost constant frequency and points of **A** and **C** are in the stable conditions just before and after the oscillation. Figure 5 shows the time variation of blade cavity length c along the inducer blade chord direction in one period of the oscillation, where t means the inducer blade pitch. Photos of cavitation behaviors at the conditions of **a** to **d** shown on the cavity length curve in Fig.5 are

also described in Fig.5 (a)~(d). Figure 6 shows the time variation of static head ψ_s at the various radius positions in the oscillating condition where R means the radius ratio to the inner radius of suction casing and the subscripts of 1, 2 is denoted as the inducer inlet and outlet, respectively. The horizontal axis of Figs.5 and 6 expresses time t normalized by one oscillation period T_{osc} . The observed cavity lengths and the time average static heads at each radial position in conditions just before and after the oscillation are shown on the left and right vertical axis of Figs.5 and 6. The photos of cavitation behaviors are also depicted in Fig.4 (e) and (f). The radial distributions of axial and circumferential velocities, ϕ and λ respectively, at the inducer inlet and outlet of the conditions of ①~④, pointed on the horizontal axis in Figs.5 and 6, are shown in Fig.7. The time average velocity distributions in the stable condition just before and after the oscillation are also shown in Fig.7 as dotted and broken lines, respectively.

From Figs.5~7, the behaviors of cavitation surge oscillation are explained as follows. In the condition of **A** just before the oscillation, a large back flow region with cavitation, where the static head becomes higher due to back flow from the inducer, is found at the upstream section of inducer tip side shown as a dotted line in Fig.7. In this condition, the cavity on the suction surface of inducer blade is also elongated and the tail end of the cavity approaches to the throat section, formed by adjacent blades. From the fact that the oscillation occurs when NPSH is slightly decreased, it is conjectured on occurring the oscillation that the blockage effect of the blade cavity elongation on the throat sectional area becomes fluctuated and this fluctuation must make the inlet flow around the blade leading edge unstable.

In the oscillating condition of **B**, the back flow at the inlet region of inducer tip is increased and decreased in one period as can be seen in Fig.7, while the time variation of outlet flow distribution is not so large in one period of the oscillation. When the back flow region is the narrowest, the blade cavity is the most elongated as the point **b** in Fig. 5 and the static head becomes uniform radially as shown in Fig.6. At that time the back flow cavitation disappear as found in Fig.5(b). Thereafter, The blade cavity is rapidly decreased for dimensionless time of 0.3, as found in Fig.5, and the back flow region is increased. Then at the point of **d**, the blade cavity becomes shorter than the throat section and the inlet back flow region with cavitation is the largest. Looking at the radial distribution of outlet flow, the axial velocity distribution is almost constant while that of the circumferential velocity is changed a little in accordance with the blade cavity length.

In the condition of **C** just after the oscillation, a narrow back flow region with cavitation is observed at the upstream section of inducer tip side, shown as a broken line in Fig.7. The blade cavity grows near the blade trailing edge as same as at the point **b** in the oscillating condition. It is conjectured on the disappearance of the oscillation as follows. During the oscillation the tail end of the blade cavity is moved up- and downstream of

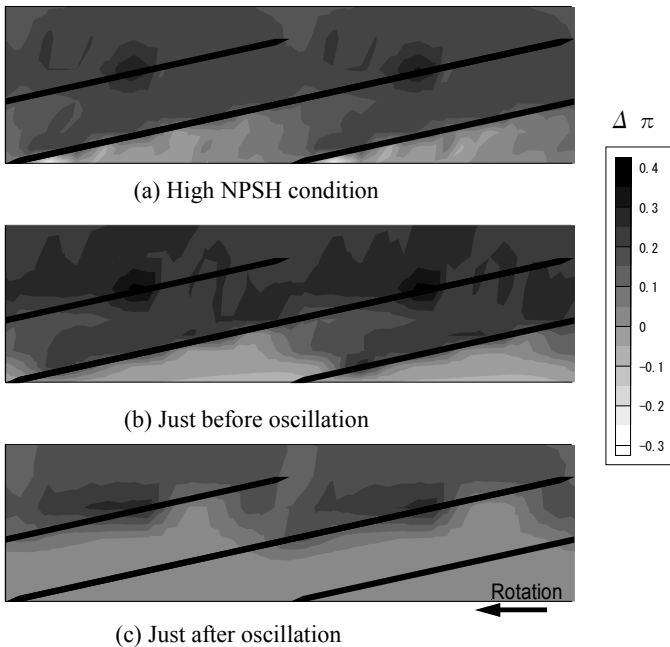


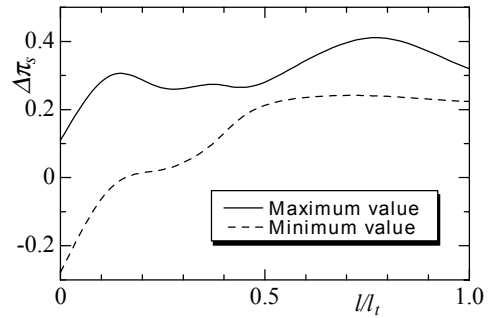
Fig.8 Blade to blade distribution of casing wall pressure

the throat section in one period. Therefore, the inlet flow at the throat section is unstable and the oscillation is remained. With decreasing NPSH, the blade cavity is gradually elongated and the tail end of the cavity is always kept downstream of the throat section. As the result, the inlet flow becomes so stable that the oscillation is ended.

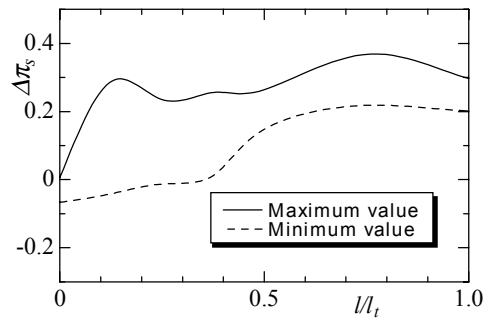
3.3 Estimate of blade force in low frequency oscillation

It was found from Figs.5~7 in the foregoing section that the oscillating flow pattern is varied between the steady ones just before and after the oscillation. This result demonstrates that the maximum and the minimum values of blade forces in one period of the oscillation can be estimated from those steady ones. Hereon it is tried to evaluate pressure distributions on the blade surface of the inducer tip from measured static heads on the casing wall in conditions just before and after the oscillation.

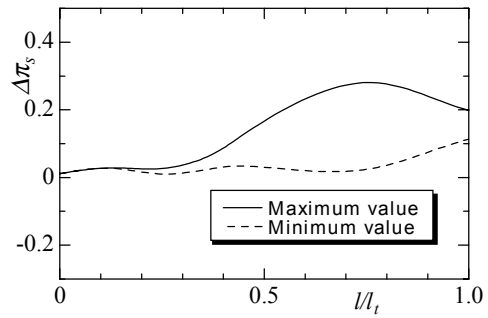
Figure 8 shows the blade to blade distributions of casing wall static head in various NPSH conditions. $\Delta\pi$ in Fig.8 is denoted as the dimensionless static-head rise from that at section ① in Fig.2. In the high NPSH condition (Fig.8 (a)), the low head zone appears near the inlet region of blade suction surface, where the tip vortex cavitation is observed. Static head is gradually increased with iso-head lines normal to blade suction surface along the blade chord direction in the semi-bladed zone upstream of the inlet throat section. In the inlet region of fully bladed zone through the throat section, consisting of adjacent blades, the head is abruptly increased. The effective blade length contributing the static head rise takes about $0.2 l_t$, where l_t is expressed as the chord length of blade tip. Though the head difference is observed between the pressure and suction surfaces in the rear passage of fully bladed zone in Fig.8 (a), the head takes almost constant in blade chord direction. The maximum static head appears at the position of $0.75 l_t$ from the leading edge on the blade



(a) High NPSH condition



(b) Just before oscillation



(c) Just after oscillation

Fig. 9 Change of pressure distributions on blade surface

pressure surface. In the NPSH condition just before the oscillation (Figs.8 (b) and 5 (e)), the tail end of blade cavity on the suction surface approaches to the throat section of the inlet. The steep head rise gradient is found in the short distance downstream of the throat section in Fig.8 (b). The head distribution in downstream passage of fully bladed zone is not changed from that in high NPSH condition. Therefore, the inducer head is kept high even in this condition of low NPSH as shown in Fig.3. As the tail end of the blade cavity is unstable and is located near the throat section, the three dimensional inlet flow with back flow becomes unstable due to the expansion and contraction of the blade cavity with scarcely decreasing NPSH. In the NPSH condition just after the oscillation (Figs.8 (c) and 5 (f)), the main part of the fully bladed zone is covered with cavitation and the static head rises at the rear part of it and on the blade pressure surface in the downstream semi-bladed zone.

Figure 9 depicts the static head distribution on the blade surface of inducer tip, which was evaluated from measured results shown in Fig.8 as the maximum values near the pressure surface and the minimum ones near the suction surface. The horizontal axis is expressed as the dimensionless distance from the leading edge of blade normalized by the blade tip chord length l_t . In the high NPSH condition (Fig.9 (a)), the maximum head difference between the pressure and suction surfaces appears at the leading edge of blade since the test inducer is a flat plate and the flow rate is low as $m=\phi_t/\tan\beta_t=0.086$. In the NPSH condition just before the oscillation (Fig.9 (b)), the growth of the blade cavity on the suction surface restricts the static head drop there. Therefore, the static head from the leading edge to the position near the throat section almost takes a value of zero. Then the blade force is decreased in comparison with that at high NPSH. In the NPSH condition just after the oscillation (Fig.9 (c)), The zero static head rise appears in the region of 80% suction surface and 30% pressure surface from the leading edge due to the elongation of the blade cavity. The maximum head difference between both surfaces is located at l/l_t = about 0.7. It is predicted from Figs.9 (b) and (c) that in one period of the oscillation, the position of the maximum head difference between the pressure and suction surfaces is moved from the front to the rear parts of the blade. This prediction demonstrates that the repeated stress acts on the inducer blade, especially at the leading edge. Therefore in the inducer design on material strength this fact should be taken into account.

4. Concluding remarks

Flow measurement was carried out for a flat plate helical inducer to clarify the phenomena of cavitation surge oscillation. The results are summarized as follows.

- 1) The cavitation surge oscillation with low frequency occurs when the tail end of the blade cavity on the suction surface approaches to the throat section of adjacent inducer blades with decreasing NPSH.
- 2) In one period of the oscillation the flow patterns just before and after the oscillation are repeated. And the size of back flow region of the inducer tip at the inlet is largely fluctuated while that of the back flow region of the inducer hub at the outlet is not so changed.
- 3) The position of the maximum pressure difference between the pressure and suction blade surfaces is expanded in the downstream direction with decreasing NPSH. In one period of the oscillation, the position of the maximum pressure difference between both surfaces is moved repeatedly between the front and the rear parts of the blade.

Acknowledgements

A part of this research was financially supported by the Grant-in-Aid from the Ministry of Education, Sports, Culture, Science and Technology.

References

- Acosta, A. J., 1958, An Experimental Study of Cavitating Inducers, *Proc. 2nd Symp. Naval Hydrodynamics*, ONR/ACR-38, 537-557.
- Ishizaka, K, and Furukawa, A., 1998, Basic Study on Advance Detection of Cavitation Surge in Helical Inducer, *Proc. US-Japan Seminar on Abnormal Flow Phenomena in Turbomachinery*, Cavitation, 1-8.
- Ishizaka, K., *et al.*, 1990, Effects of Blade Length and Blade Number of Helical Inducers on the Cavitation

- Induced Oscillation, *Proc. 3rd Japan-China Joint Conf. on Fluid Machinery, 1*, 177-184.
- Jacobsen, J. K., 1971, Liquid Rocket Engine Turbo-pump Inducers, *NASA SP-8052*.
- Maekawa, M., *et al.*, 1997, Unsteady Interblade Pressure Distributions and Fluid forces under Rotating Cavitation. (in Japanese) *Trans. JSME, Ser.B*, **63**-605, 132-138.
- Rubin, S., 1970, Prevention of Coupled Structure-Propulsion Instability (POGO), *NASA SP-8055*.
- Takamatsu, Y., Furukawa, A. and Ishizaka, K., 1984, Method of Estimation of Required NPSH of Centrifugal Pump with Inducer, *Proc. 1st China-Japan Joint Conf. on Hydraulic Machinery and Equipment*, 253-261.
- Takahara, H., *et al.*, 1989, A Study on Flow Measurement Scheme by Stepwise Rotation of Total-Pressure Tube in Flow with Steep Velocity and Pressure Gradients. (in Japanese) *Trans. JSME, Ser.B*, **55**-510, 413-418.
- Tsujimoto, Y., *et al.*, 1997, Observations of Oscillating Cavitation of an Inducer, *Trans. ASME, J. FE*, **119**-4, 775-781.
- Watanabe, S., Yokota, K., Tsujimoto, Y. and Kamijo, K., 1997, Three-Dimensional Analysis of Rotating Cavitation in Inducers, *Proc. of JSME ICFE*, **3**, 1377-1382.
- Watanabe, T. and Kawata, Y., 1978, Research on the Oscillations in Cavitating Inducer, *IAHR Joint Symp. on Design and Operation of Fluid Machinery*, 265-274.